The Preparation of Cellulose/Collagen Composite Films using 1-Ethyl-3-Methylimidazolium Acetate as a Solvent

Min Zhang,[a] Cuicui Ding,[b] Lihui Chen,[a] and Liulian Huang [a,*]

Cellulose/collagen composite films with weight ratios of 30/1 (Blend-1) and 10/1 (Blend-2) were prepared using 1-ethyl-3-methylimidazolium acetate as a common solvent. The morphology of the films observed with a field-emission scanning electron microscope displayed a dependence on the ratio of cellulose/collagen. Collagen was successfully composited with cellulose without degradation and showed a denaturation temperature (T_d) higher than that of native collagen. Fourier transform infrared spectroscopy suggested that there were hydrogen-bond interactions between collagen and cellulose in the regenerated composite films. Thermogravimetric analysis revealed that the maximum decomposition temperature (T_{max}) of cellulose decreased after regeneration, while the T_{max} of Blend-1 increased; however, it was reduced again for Blend-2. Elastic moduli from dynamic mechanical analysis exhibited a trend similar to that of T_{max}. As indicated by X-ray diffraction, the distance between cellulose molecular chains was shortened for Blend-1 and elongated for Blend-2. Furthermore, the crystallization indices were calculated to be 75.3%, 68.3%, 66.2%, and 55.4% for native cellulose, regenerated films of cellulose, Blend-1, and Blend-2, respectively. These results confirm the dependence of the structural properties of composite films on cellulose/collagen ratios through the interactions between cellulose and collagen.

Keywords: Cellulose; Collagen; Ionic liquid; Blend

*Contact information: a: College of Materials Engineering, Fujian Agriculture and Forestry University, Fuzhou 350002, PR China; b: The Key Laboratory of Leather Chemistry and Engineering of Ministry of Education, Sichuan University, Chengdu 610065, PR China; *Corresponding author: fafuhll@163.com*

INTRODUCTION

Type I collagen, which is the major component of extracellular matrices, has become a popular biomaterial and has been used widely in food, pharmacy, cosmetics, and tissue engineering due to its edibility, biocompatibility, and biodegradability (Kołodziejska *et al.* 1999; Gómez-Guillén *et al.* 2011). However, there exist some drawbacks in its properties, such as relatively low mechanical strength and thermal stability, which limit the application of collagen-based materials. One of the primary efforts devoted to improving the properties of collagen is the preparation of collagen-based composites with other polymers (mostly synthetic polymers), such as in collagen/poly(vinyl pyrrolidone) blended films (Sionkowska *et al*. 2006), PVA/collagen blends (Sarti and Scandola 1995), engineered collagen/PEO nanofibers and fabrics (Huang *et al*. 2001), and nanofibrous PLGA/collagen blends (Jose *et al*. 2009). Some properties of collagen materials, especially their mechanical strength, could be effectively improved by mixing collagen with synthetic polymers; additionally, the relatively poor biocompatibility and biodegradability of synthetic polymers limits their application in the

modification of collagen; therefore, interest has been attracted to natural polymers, which exhibit good biocompatibility and biodegradability (Kim *et al*. 2008; Boland *et al.* 2004; Lv *et al.* 2005).

Cellulose is the most abundant natural polymer and has been widely used in fields such as medical applications due to its biocompatibility, biodegradability, and desirable mechanical properties (Pinkert *et al*. 2009; Itävaara *et al*. 1999; Müller *et al*. 2006). Therefore, binary blends of natural polymers including cellulose and collagen are promising systems for creating new polymer materials with improved properties, such as thermal stability and mechanical properties. For instance, collagen and cellulose nanofiber based composites were prepared by solution casting, followed by pH-induced *in-situ* partial fibrillation of collagen phase and crosslinking of collagen phase using glutaraldehyde (Mathew *et al*. 2012). Blended films were obtained by mixing cellulose into the "collagen dough" and the mechanical properties, film structure, and composition of the collagen-cellulose composite films were characterized (Steele *et al*. 2013).

It is well known that cellulose is different from collagen in that it is insoluble in water or conventional organic solvents because of its well-developed intermolecular hydrogen bonding. Therefore, the dispersion of the two macromolecules is not easy to control in heterogeneous systems. To gain a better compatibility, a common solvent in which both collagen and cellulose could be dissolved should therefore be employed. Ionic liquids (ILs) are a group of salts that exist in liquid state at relatively low temperatures, and have been developed as a new class of green solvent for many natural polymers (Mantz *et al*. 2007). The use of ILs as cellulose solvents was first reported in 2002 (Swatloski *et al*. 2002), and the processing of cellulose using ILs has been widely studied since then (Murakami *et al*. 2007; Feng and Chen 2008; Kosan *et al*. 2008; Kuzmina *et al*. 2012). Unique mixtures of polymers in ILs, for example, mixtures of cellulose with other natural polymers, such as starch, chitosan, and lignin, have been produced (Kuzmina *et al*. 2012; El Seoud *et al*. 2007; Wu *et al*. 2009). Compared with cellulose, however, the treatment of collagen using ILs has been much less studied. In one study, collagen was dissolved in 1-butyl-3-methylimidazolium chloride ([Bmim]Cl) and the regenerated collagen was partially characterized (Meng *et al*. 2012).

Recently, collagen/cellulose hydrogel beads were reconstituted from [Bmim]Cl and were used for Cu(II) adsorption (Wang *et al*. 2013). Nevertheless, in their work, the dissolution of collagen was conducted at a relatively high temperature (> 100 °C), which probably caused damage to the native three parallel, left-handed helice because the denaturation temperature (T_d) of collagen is < 37 °C (Leikina *et al*. 2002). To prevent the denaturation of collagen during the dissolution, IL with a better dissolving capacity should be employed. With previous selections, it was found that 1-ethyl-3-methylimidazolium acetate ([Emim]Ac) was one of a number of promising alternatives as a collagen solvent at lower temperatures ([Bmim][PF6], [Bmim][BF4], [Bmim][Tf2N], [C*n*mim][PF6] and [C*n*mim][BF4]. The listed ILs are reported to have low viscosity at room temperature, such that they may be regarded as promising alternatives (Pinkert *et al*. 2009)). [Emim]Ac with solute has a relatively low viscosity; another advantage is that [Emim]Ac melts at a temperature well below room temperature (melting point < -20 °C) (Hermanutz *et al.* 2008). Recently, the dissolution of collagen in [Emim]Ac in the temperature range of 25 to 45 °C has been studied, and it was suggested that the solubility of collagen in [Emim]Ac at 25 °C reached up to 3.1 wt% (Hu *et al*. 2013).

To facilitate the process of producing blended materials for the purpose of biomedical applications such as wound dressings and scaffolds, in this work, cellulose/

collagen films were prepared by the direct dissolution of collagen in [Emim]Ac at a low temperature. The properties of the cellulose/collagen films and the interactions between the two macromolecules were investigated using several methods, including a field-emission scanning electron microscope (FESEM), thermogravimetric analysis (TGA), dynamic mechanical analysis (DMA), Fourier transform infrared spectroscopy (FTIR), and X-ray diffraction (XRD).

EXPERIMENTAL

Materials

Collagen was prepared from calf skins by the method described previously (Zhang *et al*. 2011). Briefly, the supernatants extracted from the delimed and neutralized bovine split pieces with 0.5 M acetic acid containing 3 wt% pepsin (1:3000) were collected by refrigerated centrifugation at 9000 rpm.

The supernatants were then salted out by the addition of NaCl to a final concentration of 0.7 M, and the precipitate was dissolved in 0.5 M acetic acid again and dialyzed against 0.1 M acetic acid for 3 days. Finally, pepsin-soluble collagen solution was lyophilized using a freeze dryer (Labconco FreeZone 6 Liter, USA) at -50 °C for 2 days and stored at 4 °C until used. Microcrystalline cellulose was purchased from Aladdin Co., Ltd, China. [Emim]Ac was provided by Lanzhou Institute of Chemical Physical, China.

Preparation of Regenerated Films

Ten grams of [Emim]Ac was charged into a 25-mL dried beaker with a magnetic stirrer. Microcrystalline cellulose (0.6 g) was added to the [Emim]Ac. The dissolving process was controlled at 60 °C for 4 h, and a clear solution was obtained. After the solution was cooled, collagen sponge was added (the doses of collagen were 0.02 and 0.06 g, for cellulose/collagen ratios of 30/1 and 10/1 (w/w), respectively). The following dissolving process was controlled at 25 °C for 6 h. The cellulose/collagen blends with ratios of 30/1 and 10/1 were named Blend-1 and Blend-2, respectively.

The [Emim]Ac with cellulose or collagen/cellulose was cast on a film blade and was then soaked in deionized water, which was renewed every 0.5 h for a total of 4 times. To keep collagen from becoming denatured, the whole regeneration process was carried out at 4 °C. [Emim]Ac was washed away by deionized water, and regenerated films were obtained. The regenerated films were dried in a desiccator to a constant weight and stored until use.

Field-Emission Scanning Electron Microscopy (FESEM)

The morphology of the regenerated films was examined with a field-emission scanning electron microscope (Navo FEI NanoSEM 230, USA), operated at an accelerating voltage of 15 kV.

Atomic Force Microscopy (AFM)

The surface morphology of the regenerated films was examined on the dried samples by AFM. The AFM (SHIMADZU SPM 9600, Japan) with a pinpoint (NSG 11, Russia) was operated in the dynamic mode at room temperature (~20 °C). Each sample was scanned with a scanning rate of 1 Hz.

Ultraviolet (UV) Spectroscopy

The UV adsorption spectrum of the regenerated films was examined utilizing a spectrophotometer (Hitachi U-2001, Japan) with an integrating sphere. The incident angle was 0°, the spectral slit width was 50 nm, and the scanning wavelength range was from 200 to 400 nm.

Differential Scanning Calorimetry (DSC)

The thermal stability of collagen in the regenerated films was evaluated by DSC (Netzsch DSC 200PC, Germany). The samples were weighed accurately into aluminum pans, sealed, and then scanned from 20 to 180 °C at a heating rate of 10 °C/min in a N_2 atmosphere. Liquid nitrogen was used as a cooling medium, and empty pans were used as the reference.

Fourier Transform Infrared Spectroscopy (FTIR)

FTIR spectra of the samples were recorded with a FTIR spectrophotometer (Thermo Scientific Nicolet IS10, USA) using potassium bromide (KBr) pellets. The measurements were performed at a data acquisition rate of 4 cm^{-1} per point and in the range of 500 to 4000 cm^{-1}. A total of 32 scans were performed for each sample.

Thermogravimetric Analysis (TGA)

TG analysis of the samples was carried out using a thermal analyzer (Netzsch TG 209, Germany). Samples of 2 to 3 mg were heated under a N_2 atmosphere from 40 to 600 °C at a heating rate of 10 °C/min.

Dynamic Mechanical Analysis (DMA)

The elastic moduli of the samples (20.0 × 5.0 mm^2) were measured as a function of temperature using a DMA analyzer (Netzsch DMA 242C, Germany). The thickness of regenerated films of cellulose, Blend-1, and Blend-2 was 35, 36, and 36 μm, respectively, measured from at least three different regions of films. The testing was conducted at a constant frequency of 1 Hz from 30 to 180 °C with a heating rate of 3 °C/min. The environmental chamber was purged with dry N_2.

X-Ray Diffraction (XRD)

X-ray powder diffraction measurements of the samples were performed using a diffractometer (Panalytical X'pert Pro MPD, Netherlands) at a scanning rate of 1°/min in the 2θ range from 5 to 59°, with a 0.2-mm Ni filter plate and Cu Kα radiation (λ=0.154056 nm).

RESULTS

FESEM and AFM Images of Regenerated Films

As seen in the FESEM images (Fig. 1), the surface of regenerated cellulose (Fig. 1a) was not smooth and displayed some microgrooves, while the regenerated Blend-1 (Fig. 1b) exhibited a compact and smooth morphology. As for the regenerated Blend-2 (Fig. 1c), however, the surface became rough again. It seemed that the morphology of the regenerated composite films exhibited a dependence on the cellulose/collagen ratio.

To further observe these films in the nanometer range, AFM was performed (Fig. 2). From AFM images, it seemed that the regenerated cellulose film was formed by spherical nanodomains or clusters and the surface of the film was rough (Fig. 2a). The fiber fines of collagen were staggered in the clusters of cellulose and a compact as well as smooth surface morphology was observed for Blend-1 (Fig. 2b). As for Blend-2, however, some clusters of collagen appeared and thus again the surface became rough (Fig. 2c). Morphologies observed from AFM images of the three samples were quite in line with those observed from SEM.

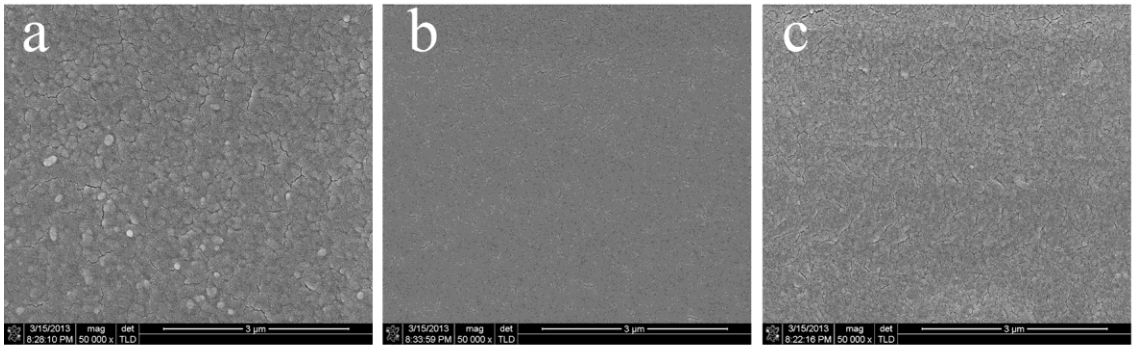

Fig. 1. FESEM images of regenerated films of (a) cellulose, (b) Blend-1, and (c) Blend-2

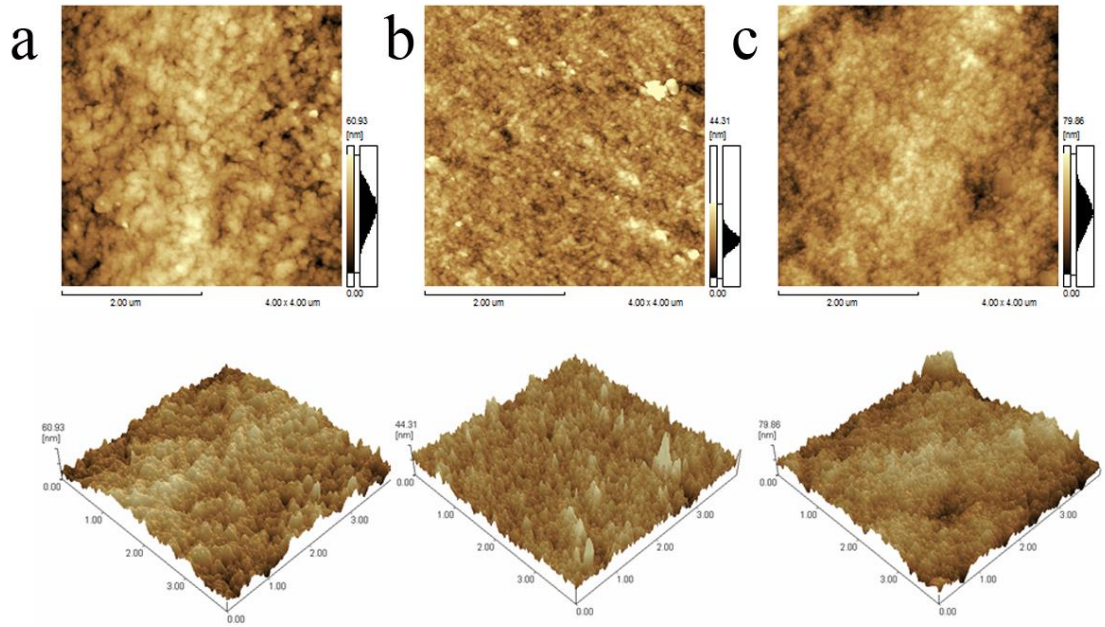

Fig. 2. AFM images (the upper is height map and the bottom is three-dimensional map) of regenerated films of (a) cellulose, (b) Blend-1, and (c) Blend-2

Ultraviolet (UV) Spectroscopy of Regenerated Films

Collagen exhibited a weaker film-forming ability compared with cellulose; thus, the collagen content was limited to 10 wt% in the blends. To ensure the existence of collagen in the regenerated films, the UV spectra of the films was examined and analyzed. As seen in Fig. 3, the regenerated cellulose film had an absorption near 227.5

nm, while the regenerated film of Blend-1 had two absorptions: 225 and 284.5 nm. A blue shift occurred as the content of collagen increased; that is, the absorptions of the regenerated film for Blend-2 shifted to lower wavelengths: 218 and 280 nm. Tyrosine and phenylalanine are sensitive chromophores and absorb UV light at 283 and 251 nm (Doyle and Bello 1968). The absorption at ~280 nm therefore suggests the existence of collagen in the regenerated films of Blend-1 and Blend-2. The blue shift of the ~280 nm peak is probably due to the enhancement of intermolecular hydrogen bonding among collagen molecules or between collagen and cellulose molecules (Manna *et al*. 2006).

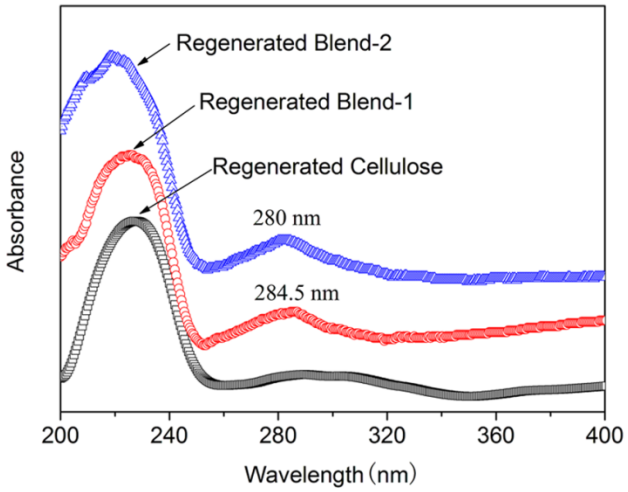

Fig. 3. UV spectroscopy of regenerated films of cellulose, Blend-1, and Blend-2

DSC Thermograms

As shown in Fig. 4, there was no obvious endothermic peak for the regenerated cellulose film, while the regenerated films for Blend-1 and Blend-2 exhibited endothermic peaks at 81.2 and 92.8 °C, respectively.

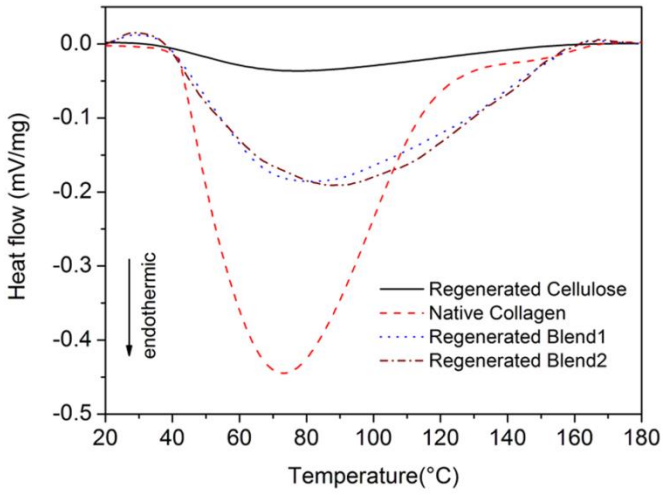

Fig. 4. DSC thermograms of native collagen and regenerated films of cellulose, Blend-1, and Blend-2

The denaturation temperatures of collagen in both Blend-1 and Blend-2 were higher than that of the native collagen film (73.4 °C). This suggests that the thermal stability of collagen was improved by its interaction with cellulose. The collagen was subjected to the process of dissolution and regeneration in [Emim]Ac at 25 °C. The higher T_d of regenerated Blend-2 than that of regenerated Blend-1 indicated the enhanced interaction between collagen and cellulose, as the collagen content in the regenerated Blend-2 film was greater.

FTIR Analysis

Figure 5 shows the FTIR spectra for the native cellulose and regenerated films. Figure 5I(a) displays the characteristic peaks of cellulose, primarily at 1641, 1430, 1372, 1163, 1115, 1064, 1059, and 899 cm^{-1}. The peak at 1641 cm^{-1} is attributed to the absorption of linked water residue in the samples (Sun *et al*. 2001). The peaks at 1372 cm^{-1} and 1430 cm^{-1} indicate CH_2 and OH bending and C–H and OH bending, respectively. The bands at 1163 cm^{-1}, 1115, and 1059 cm^{-1} represent C–O and C–O–C stretching and some C–OH bending. The prominent band at 1064 cm^{-1} represents ring vibration and C–OH bending. An absorption band at ~899 cm^{-1} indicates β-glycosidic linkages (Sun and Hughes 1998).

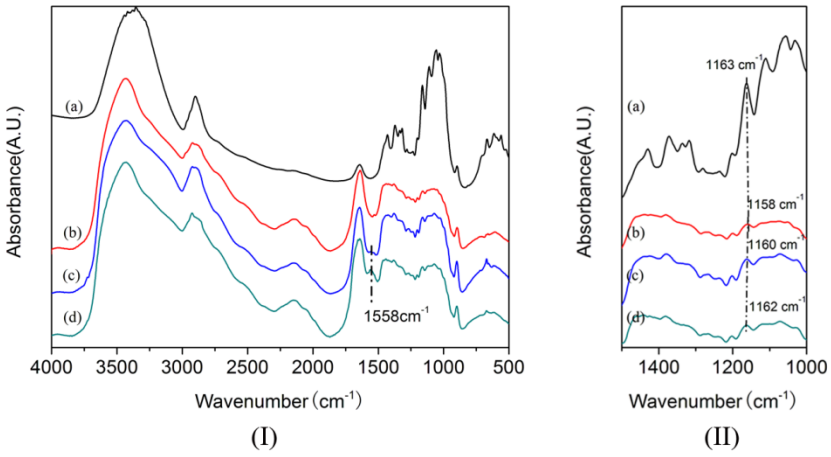

Fig. 5. (I) FTIR spectra in the range of 4000 to 500 cm^{-1} for (a) cellulose, (b) regenerated cellulose, (c) regenerated Blend-1, and (d) regenerated Blend-2; (II) FTIR spectra in the range of 1500 to 1000 cm^{-1}

As for the regenerated cellulose film in Fig. 5I(b), however, the characteristic peaks in the range of 1500 to 1000 cm^{-1} were weaker than those of native cellulose. The FTIR spectra of Blend-1 was similar to that of regenerated cellulose, except for a new peak located at ~1558 cm^{-1}, as shown in Fig. 5I(c). The appearance of this new peak is associated with the amide II of collagen molecules (Muyonga *et al*. 2004). Moreover, as the collagen content increased (Blend-2), the intensity of this new peak increased and shifted to higher wavenumbers, *i.e.*, ~1560 cm^{-1} (Fig. 5I(d)), which could be attributed to the change in the interaction among amide groups (Wang *et al*. 2013). As shown in Fig. 5II, the bands at 1163 cm^{-1}, assigned to C–O, C–O–C stretching, and some C–OH bending, shifted to lower wavenumbers (1158 cm^{-1}) in comparison with those of the native cellulose, indicating that the destruction of intermolecular hydrogen bonds involving the exocyclic hydroxyl groups (O_6) occurred (Liu *et al*. 2010). As collagen was

added, however, this band shifted to higher wavenumbers (1160 and 1162 cm^{-1} for Blend-1 and Blend-2, respectively), suggesting that intermolecular hydrogen bonds were enhanced to a certain level due to the addition of collagen.

The changes in the characteristic peaks of the FTIR spectra demonstrated that there were hydrogen-bond interactions between collagen and cellulose in the composite films, as collagen, which is a hydrogen donor, would form hydrogen bonds with the hydroxyl groups of cellulose.

TG Thermograms

The TG thermographs (a) and the DTG curves (b) for all the samples are shown in Fig. 6. From the DTG curves, the corresponding temperature (T_{max}) of the maximum decomposition rate could be obtained. Rapid decomposition in a narrow temperature range of 350 to 360 °C was observed for the initial cellulose sample. T_{max} for the native cellulose (359.6 °C) was higher than that of the native collagen (324.7 °C), indicating that the thermal stability of the native cellulose is superior to that of native collagen.

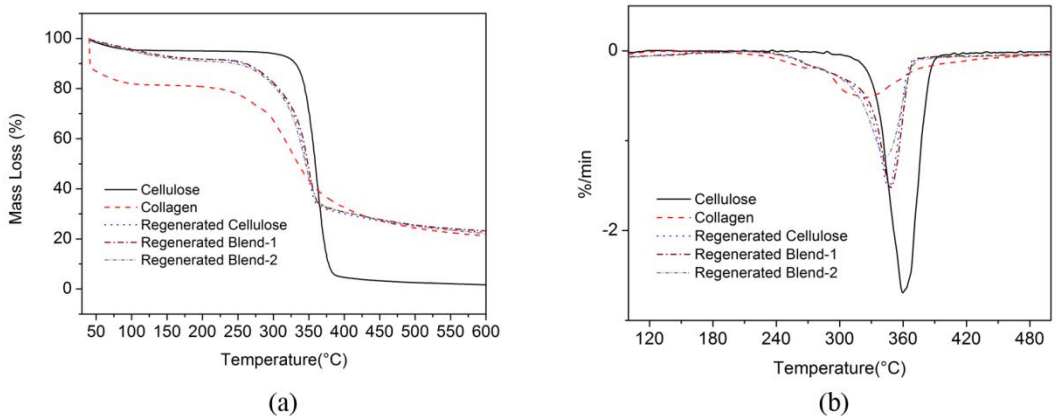

Fig. 6. Thermal decomposition profiles (a) and derivative curves (b) of native cellulose, collagen, and regenerated films

The regenerated cellulose film had a T_{max} value of 345.8 °C, which was 13.8 °C lower than that of native cellulose; however, it gives a higher char yield on pyrolysis, as indicated by the high residual masses after the decomposition step, which were similar to previously reported results (Swatloski *et al*. 2002). The reduction in the thermal stability of cellulose might be related to the fact that it underwent degradation during dissolution, leading to the loss of the crystalline structure of cellulose (Mahadeva and Kim 2009). As for regenerated Blend-1, however, T_{max} slightly increased to 348.7 °C, indicating that the thermal stability of the composite film was improved. It was found that films blended from cellulose and chitosan had a thermal stability higher than that of the original polysaccharides and the strong interactions between the polysaccharides in the blend were thought to be the reason of the higher temperatures of degradation (Kuzmina *et al*. 2012). Therefore, the improvement in T_{max} of Blend-1 could also be considered to be related to the interactions between the collagen and cellulose molecules. In contrast, in the case of regenerated Blend-2, T_{max} was reduced to 342.4 °C, even lower than that of the regenerated cellulose film, implying that the interactions among cellulose molecules might be blocked by the excess addition of collagen.

DMA of Regenerated Films

The elastic moduli (*E′*) curves of the samples as a function of temperature determined by DMA are shown in Fig. 7. It has been suggested that there are correlations between temperature-dependent elastic moduli of epoxies measured by DMA and mechanical testing data (Deng *et al*. 2007); therefore, the elastic moduli obtained for regenerated films (Fig. 7a) also reflect the mechanical strength of the films. In the range of 30 to 180 °C, the values of *E′* for all the samples first increased to reach a maximum, and then decreased with increasing temperature. At the same temperature, regenerated Blend-1 possessed an *E′* higher than that of regenerated cellulose, while regenerated Blend-2 had an *E′* lower than that of regenerated cellulose. This shows that the mechanical strength of the composite film improved with the addition of only a small amount of collagen, while more collagen decreased the mechanical strength. The increase in mechanical properties was observed to be remarkable in the composites of collagen and cellulose nanofibers, and the key to the synergistic improvement was thought to be attributed to the high surface area of nanosized cellulose fibers as well as collagen nanofibers, which provides a highly entangled physical network (Mathew *et al*. 2012). The increase in *E′* of Blend-1 could also be ascribed to the interactions between collagen and cellulose.

The curves of viscous moduli as a function of temperature (Fig. 7(b)) suggested that all three samples tended to exhibit a viscous behavior with the increase of temperature. However, at the same temperature, regenerated Blend-1 possessed *E″* higher than that of regenerated cellulose, while regenerated Blend-2 had *E″* lower than that of regenerated cellulose, which was consistent with the trend of the variation of *E′* observed from Fig. 7(a).

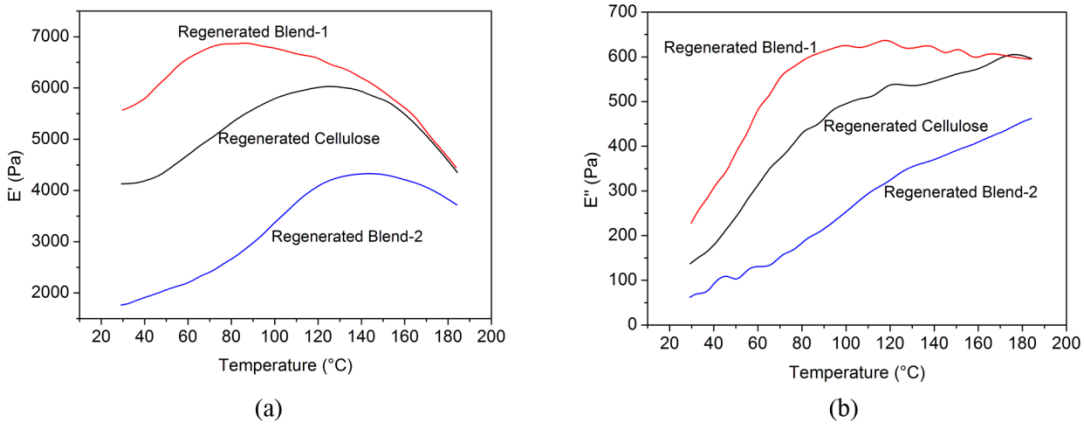

Fig. 7. The elastic moduli (*E′*) and viscous moduli (*E″*) curves of samples determined by DMA

XRD Characterization

XRD has been extensively used to investigate the supramolecular order of cellulose fibers (Cunha *et al*. 2007). The structure of the native cellulose fiber and regenerated films was examined with XRD (Fig. 8). The native cellulose shows typical diffraction peaks at 2θ = 16.2°, 22.6°, and 34.5°, which were assigned to 101, 002, and 040 peaks, respectively (Takegawa *et al*. 2010; Zhao *et al*. 2007). After dissolution and subsequent coagulation with water, the regenerated cellulose film exhibited diffraction peaks at 2θ = 11.7°, 20.4°, and 35.2°. The changes in the diffraction peaks can be ascribed to the conversion of cellulose I (native cellulose) to cellulose II (regenerated

cellulose) that occurred during dissolution and regeneration (Liu *et al*. 2010). The regenerated Blend-1 shows diffraction peaks at 2θ = 12.7° and 20.9°, and those of the regenerated Blend-2 were at 12.2° and 21.3°. According to the location of the 101 peak and the Bragg diffraction equation (Jia *et al*. 2008),

$$2d\sin\theta = 0.154056 \text{ nm} \quad (1)$$

the distances between the molecular chains of cellulose were calculated to be 0.547, 0.756, 0.696, and 0.725 nm for the native cellulose, regenerated cellulose film, and regenerated films of Blend-1 and Blend-2, respectively. This result indicated that the distances between the molecular chains of cellulose increased after the dissolution and regeneration, probably due to the partial removal of the hydrogen-bond interactions between cellulose molecules; however, the distance between the molecular chains of cellulose was shortened with the addition of a small amount of collagen (Blend-1), while the distance between molecular chains became large again as the amount of collagen further increased (Blend-2).

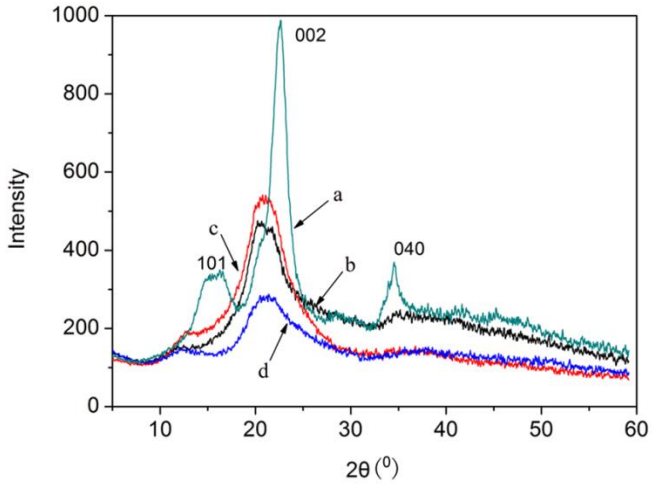

Fig. 8. XRD diagrams of samples: (a) native cellulose, (b) regenerated cellulose, (c) regenerated Blend-1, and (d) regenerated Blend-2

Crystallization index (CI) is another important parameter to describe the supramolecular structure of materials. It is calculated as the height ratio between the intensity of the crystalline peak (I_{002} - I_{AM}) (I_{002}: the height of the 002 peak; I_{AM}: the height of the minimum between the 002 and 101 peaks) and the total intensity (I_{002}) after subtraction of the background signal (Park *et al*. 2010). According to this method, the CIs were calculated to be 75.3%, 68.3%, 66.2%, and 55.4% for the native cellulose, regenerated films of cellulose, Blend-1, and Blend-2, respectively. This reveals that the CI of cellulose was reduced after the dissolution and regeneration in IL, and a small quantity of collagen (0.02 g) did not obviously influence the value of CI for the regenerated cellulose; however, a further increase in collagen content remarkably decreased the value of the CI. This result further confirmed that the hydrogen-bond interactions among cellulose molecules may be disturbed after the dissolution in IL or by the addition of a large amount of collagen (0.06 g).

DISCUSSION

The dissolution mechanism of cellulose in ILs has been previously explored (Feng and Chen 2008). Cellulose acts as an electron pair donor, and hydrogen atoms serve as electron acceptors, while the cations in IL solvents act as the electron acceptor center and anions in the solvents act as the electron donor center. Through the interaction between hydroxyl groups (in cellulose) and IL, the oxygen and hydrogen atoms of the hydroxyl groups are separated, resulting in the opening of the hydrogen bonds among molecular chains of cellulose, causing the cellulose to dissolve. Similarly, the mechanism of dissolution and regeneration of collagen in the [Emim]Ac solvent system has been previously explored: [Emim]Ac first disrupts the hydrogen bonds between intermolecules or intramolecules, and then the hydrogen bonds are rebuilt after the removal of [Emim]Ac (Hu *et al*. 2013). By combining these previously proposed mechanisms with the results in this experiment, the possible mechanism of the dissolution, regeneration, and composite formation of collagen and cellulose in [Emim]Ac is proposed (Fig. 9). [Emim]Ac dissolved the collagen and cellulose by breaking the hydrogen bonds in collagen and cellulose molecules. During the process of regeneration, with the [Emim]Ac washed away with water, the hydrogen bonding could be rebuilt among the collagen chains or cellulose chains, or between the collagen and cellulose chains, forming the composites.

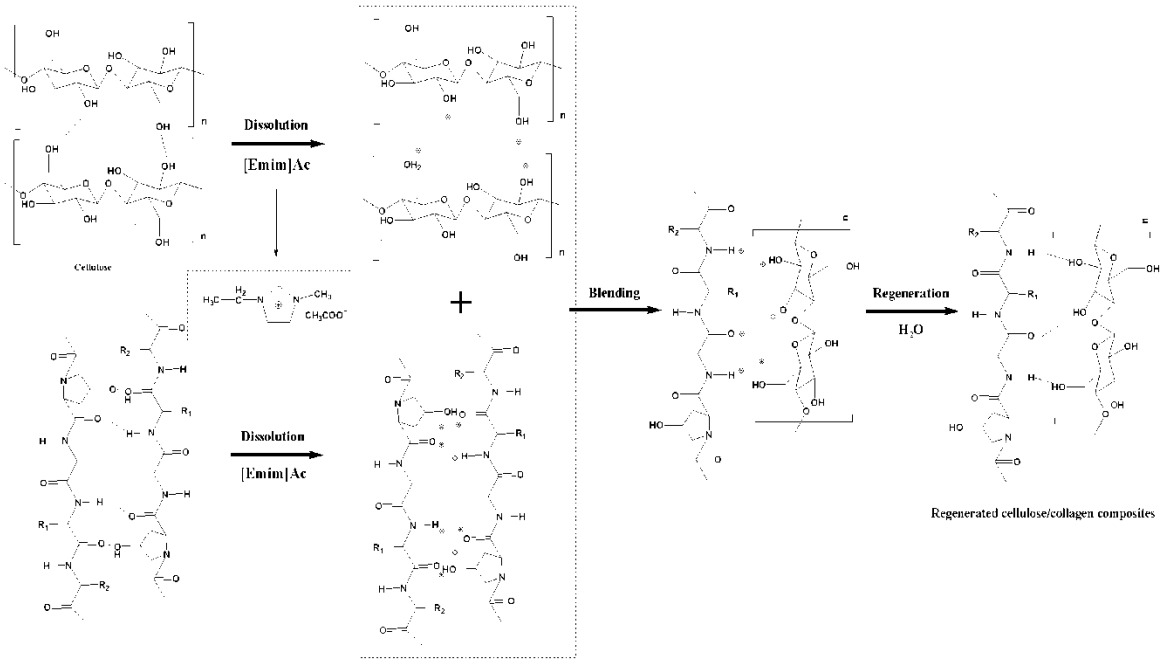

Fig. 9. The possible mechanism of the dissolution, regeneration, and composite formation of cellulose and collagen in [Emim]Ac

Therefore, according to the above results and analysis, the proposed interactions between molecules in the regenerated films with cellulose/collagen ratios of 30/1 and 10/1, respectively, could be presented as shown in Fig. 10. The hydrogen-bond interactions among cellulose molecules would be destroyed to a certain extent after dissolution in IL, and thus the CI of the regenerated cellulose film decreased and the

distance between molecular chains of cellulose was elongated (Fig. 10a). With the addition of a small amount of collagen, the hydrogen-bond interactions among cellulose molecules were not obviously influenced (CI was not noticeably reduced). Entanglement and hydrogen-bond interactions between the two macromolecules may have occurred (the distance between the molecular chains of cellulose was shortened). From results mentioned above, a synergistic effect appears to occur between entanglement and hydrogen-bond interactions, leading to a compact and smooth morphology as well as the improvement in properties such as thermal stability and mechanical strength of the composite film (Fig. 10b). As more collagen was added to the blends, the interactions among collagen itself were further enhanced (as seen from Fig. 3 and Fig. 4); however, the interactions among cellulose molecules were disturbed, and the regularity of the assembled cellulose molecules may have been damaged (CI was significantly reduced and the distance between the molecular chains of cellulose was elongated again), resulting in the relatively rough morphology and the reduction of properties such as the thermal stability and mechanical strength of the composite film (Fig. 10c).

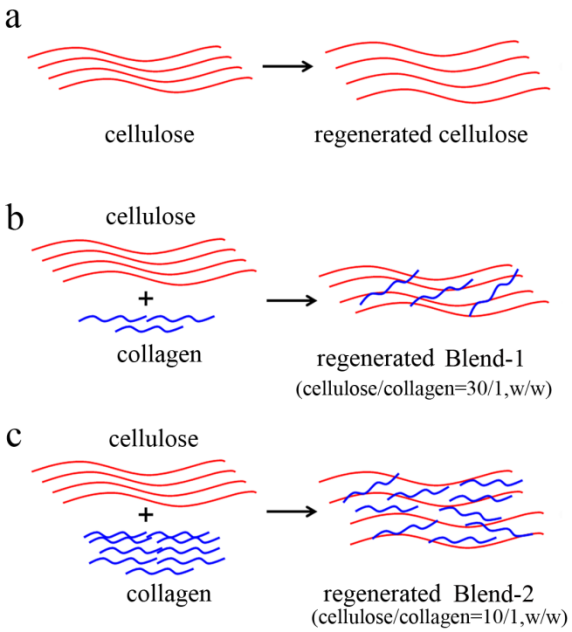

Fig. 10. Proposed interactions between molecules in the regenerated films: (a) cellulose, (b) Blend-1, and (c) Blend-2

To obtain composite films with a good compatibility between collagen and cellulose molecules, the amount of collagen in the composites was limited (cellulose/collagen > 10/1) in the present work. To prepare cellulose/collagen composite films with larger amount of collagen, a temperature higher than 25 °C (but should be lower than the T_d of collagen, 37 °C) should be employed, which could improve the solubility of collagen in [Emim]Ac. The changes of interactions between collagen and cellulose molecules in composite films with various cellulose/collagen ratios, probably including the entanglement and hydrogen-bond interaction, could be further clarified through a subsequent study.

CONCLUSIONS

1. Cellulose could be efficiently dissolved in [Emim]Ac at 60 °C. At a temperature (25 °C) lower than the T_d of collagen (37 °C), collagen could also be directly dissolved in [Emim]Ac without degradation, allowing it to be formed into composite films with cellulose.
2. Properties such as thermal stability and mechanical strength of the regenerated composite films exhibited a dependence on the cellulose/collagen ratio, which was related to the changes in interactions between collagen and cellulose molecules in the regenerated composite films.
3. As a whole, the novel cellulose/collagen composite films, which could be potentially applied as biomedical materials, could be prepared using [Emim]Ac as a common solvent of collagen and cellulose. Properties of the films could be improved by blending the two macromolecules and adjusting the cellulose/collagen ratio.

ACKNOWLEDGMENTS

This work was financially supported by the National Natural Science Foundation of China (No. 21306024), the Science and Technology Major Project of the Science and Technology Department of Fujian Province (2008HZ0001-1), and the Foundation of Distinguished Young Scholars of Fujian Agriculture and Forestry University (XJQ201212).

REFERENCES CITED

Boland, E. D., Matthews, J. A., Pawlowski, K. J., Simpson, D. G., Wnek, G. E., and Bowlin, G. L. (2004). "Electrospinning collagen and elastin: Preliminary vascular tissue engineering," *Front. Biosci*. 9, 1422-1432.

Cunha, A. G., Freire, C. S., Silvestre, A. J., Neto, C. P., Gandini, A., Orblin, E., and Fardim, P. (2007). "Characterization and evaluation of the hydrolytic stability of trifluoroacetylated cellulose fibers," *J. Colloid Interf. Sci*. 316(2), 360-366.

Deng, S., Hou, M., and Ye, L. (2007). "Temperature-dependent elastic moduli of epoxies measured by DMA and their correlations to mechanical testing data," *Polym. Test.* 26(6), 803-813.

Doyle, R., and Bello, J. (1968). "Ultraviolet absorbance changes accompanying the denaturation of soluble collagen and antelocollagen," *Biochem. Biophys. Res. Commun.* 31(6), 869-876.

El Seoud, O. A., Koschella, A., Fidale, L. C., Dorn, S., and Heinze, T. (2007). "Applications of ionic liquids in carbohydrate chemistry: A window of opportunities," *Biomacromolecules* 8(9), 2629-2647.

Feng, L., and Chen, Z. -L. (2008). "Research progress on dissolution and functional modification of cellulose in ionic liquids," *J. Mol. Liq.* 142(1), 1-5.

Gómez-Guillén, M., Giménez, B., López-Caballero, M., and Montero, M. (2011). "Functional and bioactive properties of collagen and gelatin from alternative sources: A review," *Food Hydrocolloid*. 25(8), 1813-1827.

Hermanutz, F., Gähr, F., Uerdingen, E., Meister, F., and Kosan, B. (2008). "New developments in dissolving and processing of cellulose in ionic liquids," *Macromo. Symp*. 262(1), 23-27.

Hu, Y., Liu, L., Dan, W., Dan, N., and Gu, Z. (2013). "Evaluation of 1-ethyl-3-methylimidazolium acetate based ionic liquid systems as a suitable solvent for collagen," *J. Appl. Polym. Sci*. 130(4), 2245-2256.

Huang, L., Nagapudi, K., Apkarian, R. P., and Chaikof, E. L. (2001). "Engineered collagen-PEO nanofibers and fabrics," *J. Biomater. Sci. Polym. Ed.* 12(9), 979-993.

Itävaara, M., Siika-Aho, M., and Viikari, L. (1999). "Enzymatic degradation of cellulose-based materials," *J. Environ. Polym. Degrad*. 7(2), 67-73.

Jia, G., Zheng, Y., Liu, K., Song, Y., You, H., and Zhang, H. (2008). "Facile surfactant- and template-free synthesis and luminescent properties of one-dimensional Lu_2O_3: Eu^{3+} phosphors," *J. Phys. Chem. C* 113(1), 153-158.

Jose, M. V., Thomas, V., Dean, D. R., and Nyairo, E. (2009). "Fabrication and characterization of aligned nanofibrous PLGA/collagen blends as bone tissue scaffolds," *Polymer* 50(15), 3778-3785.

Kim, T. G., Chung, H. J., and Park, T. G. (2008). "Macroporous and nanofibrous hyaluronic acid/collagen hybrid scaffold fabricated by concurrent electrospinning and deposition/leaching of salt particles," *Acta Biomater*. 4(6), 1611-1619.

Kołodziejska, I., Sikorski, Z. E., and Niecikowska, C. (1999). "Parameters affecting the isolation of collagen from squid (*Ilex argentinus*) skins," *Food Chem.* 66(2), 153-157.

Kosan, B., Michels, C., and Meister, F. (2008). "Dissolution and forming of cellulose with ionic liquids," *Cellulose* 15(1), 59-66.

Kuzmina, O., Heinze, T., and Wawro, D. (2012). "Blending of cellulose and chitosan in alkyl imidazolium ionic liquids," *ISRN Polym. Sci*. 2012, 9.

Leikina, E., Mertts, M., Kuznetsova, N., and Leikin, S. (2002). "Type I collagen is thermally unstable at body temperature," *Proc. Nat. Acad. Sci. USA* 99(3), 1314-1318.

Liu, S., Zeng, J., Tao, D., and Zhang, L. (2010). "Microfiltration performance of regenerated cellulose membrane prepared at low temperature for wastewater treatment," *Cellulose* 17(6), 1159-1169.

Lv, Q., Feng, Q., Hu, K., and Cui, F. (2005). "Three-dimensional fibroin/collagen scaffolds derived from aqueous solution and the use for HepG2 culture," *Polymer* 46(26), 12662-12669.

Müller, F. A., Müller, L., Hofmann, I., Greil, P., Wenzel, M. M., and Staudenmaier, R. (2006). "Cellulose-based scaffold materials for cartilage tissue engineering," *Biomaterials* 27(21), 3955-3963.

Mahadeva, S. K., and Kim, J. (2009). "Electromechanical behavior of room temperature ionic liquid dispersed cellulose," *J. Phys. Chem. C* 113 (28), 12523-12529.

Manna, S., Saha, A., and Nandi, A. K. (2006). "A two component thermoreversible hydrogel of riboflavin and melamine: Enhancement of photoluminescence in the gel form," *Chem. Commun*. 41, 4285-4287.

Mantz, R., Fox, D., Green, J., Fylstra, P., De Long, H., and Trulove, P. (2007). "Dissolution of biopolymers using ionic liquids," *Z. Naturforsch. A: Phys. Sci*. 62(5-6), 275-280.

Mathew, A. P., Oksman, K., Pierron, D., and Harmad, M.-F. (2012). "Crosslinked fibrous composites based on cellulose nanofibers and collagen with in situ pH induced fibrillation," *Cellulose* 19 (1), 139-150.

Meng, Z., Zheng, X., Tang, K., Liu, J., Ma, Z., and Zhao, Q. (2012). "Dissolution and regeneration of collagen fibers using ionic liquid," *Int. J. Biol. Macromol*. 51(4), 440-448.

Murakami, M.-A., Kaneko, Y., and Kadokawa, J.-I. (2007). "Preparation of cellulose-polymerized ionic liquid composite by in-situ polymerization of polymerizable ionic liquid in cellulose-dissolving solution," *Carbohyd. Polym*. 69(2), 378-381.

Muyonga, J., Cole, C., and Duodu, K. (2004). "Characterisation of acid soluble collagen from skins of young and adult Nile perch (*Lates niloticus*)," *Food Chem*. 85(1), 81-89.

Park, S., Baker, J. O., Himmel, M. E., Parilla, P. A., and Johnson, D. K. (2010). "Cellulose crystallinity index: Measurement techniques and their impact on interpreting cellulase performance," *Biotechnol. Biofuels* 3, 10.

Pinkert, A., Marsh, K. N., Pang, S., and Staiger, M. P. (2009). "Ionic liquids and their interaction with cellulose," *Chem. Rev.* 109(12), 6712-6728.

Sarti, B., and Scandola, M. (1995). "Viscoelastic and thermal properties of collagen/poly(vinyl alcohol) blends," *Biomaterials* 16(10), 785-792.

Steele, T. W., Huang, C.L., Nguyen, E., Sarig, U., Kumar, S., Widjaja, E., Loo, J. S., Machluf, M., Boey, F., and Vukadinovic, Z. (2013). "Collagen–cellulose composite thin films that mimic soft-tissue and allow stem-cell orientation," *J. Mater. Sci. - Mater. Med.* 24(8), 2013-2027.

Sionkowska, A., Wisniewski, M., Kaczmarek, H., Skopinska, J., Chevallier, P., Mantovani, D., Lazare, S., and Tokarev, V. (2006). "The influence of UV irradiation on surface composition of collagen/PVP blended films," *Appl. Surf. Sci*. 253(4), 1970-1977.

Sun, R., Fang, J., Tomkinson, J., Geng, Z., and Liu, J. (2001). "Fractional isolation, physico-chemical characterization and homogeneous esterification of hemicelluloses from fast-growing poplar wood," *Carbohyd. Polym*. 44(1), 29-39.

Sun, R., and Hughes, S. (1998). "Fractional extraction and physico-chemical characterization of hemicelluloses and cellulose from sugar beet pulp," *Carbohyd. Polym*. 36(4), 293-299.

Swatloski, R. P., Spear, S. K., Holbrey, J. D., and Rogers, R. D. (2002). "Dissolution of cellulose with ionic liquids," *J. Am. Chem. Soc*. 124(18), 4974-4975.

Takegawa, A., Murakami, M.-A., Kaneko, Y., and Kadokawa, J.-I. (2010). "Preparation of chitin/cellulose composite gels and films with ionic liquids," *Carbohyd. Polym.* 79(1), 85-90.

Wang, J., Wei, L., Ma, Y., Li, K., Li, M., Yu, Y., Wang, L., Qiu, H., Wang, L., and Qiu, H. (2013). "Collagen/cellulose hydrogel beads reconstituted from ionic liquid solution for Cu (II) adsorption," *Carbohyd. Polym*. 98(1), 736-743.

Wu, R.-L., Wang, X.-L., Li, F., Li, H.-Z., and Wang, Y.-Z. (2009). "Green composite films prepared from cellulose, starch and lignin in room-temperature ionic liquid," *Bioresour. Technol*. 100(9), 2569-2574.

Zhang, M., Wu, K., and Li, G. (2011). "Interactions of collagen molecules in the presence of N-hydroxysuccinimide activated adipic acid (NHS-AA) as a crosslinking agent," *Int. J. Biol. Macromol*. 49(4), 847-854.

Zhao, H. B., Kwak, J. H., Zhang, Z. C., Brown, H. M., Arey, B. W., and Holladay, J. E. (2007). "Studying cellulose fiber structure by SEM, XRD, NMR and acid hydrolysis," *Carbohyd. Polym*. 68(2), 235-241.

Article submitted: September 23, 2013; Peer review completed: November 28, 2013; Revised version received and accepted: December 12, 2013; Published: December 16, 2013.